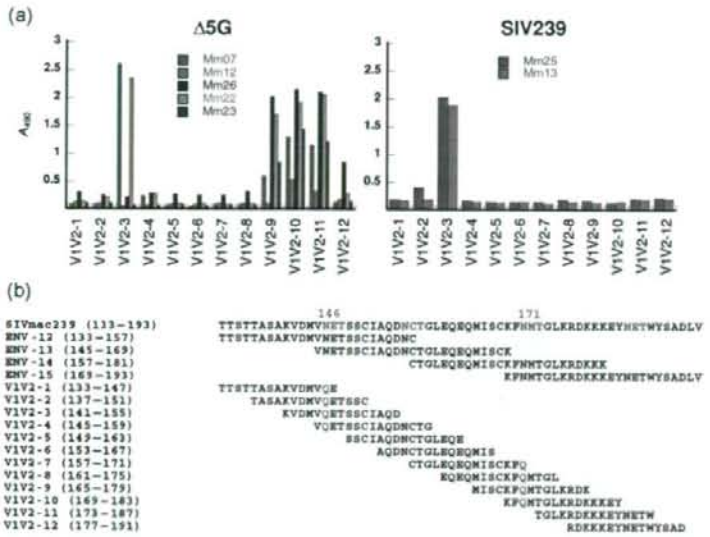

Fig. 5. Ab reactivity to linear epitopes in the V1/V2 region of gp120. (a) To define linear epitopes in the V1/V2 region, peptide ELISA was performed using 12 peptides (15 mers) overlapping by 11 residues each. (b) Sequences and positions of the 12 V1/V2 peptides used in (a) and the peptides Env-12 to -15.

peptide was not detected in any samples, confirming that the epitopes targeted by nAb and V1V2-specific Ab were distinct (data not shown).

Next, we tested plasma IgG samples from SIV-infected animals for the quantitative capture of whole virions. IgG fractions of plasma samples from SIV-infected animals collected at 3–4 weeks p.i. were compared for their capacity to capture Δ5G or SIV239 virions. IgG fractions from two Δ5G-infected animals (Mm07 and Mm22) exhibited remarkably higher virion capture activity than those from other animals (Fig. 7a); however, this capture activity was

Table 1. Epitope-specific Ab-binding regions in Env and influence of deglycosylation on Ab binding

Env subunit	Ab-binding region	Peptide no.	Amino acid range	Region	*P* value*
SU	Region 1	10	109–133	V1	0.6733
		12	133–157	V1	0.5678
		13	145–169	V1/V2	0.5563
		14	157–181	V1/V2	0.0149†
		15	169–193	V1/V2	0.2385
	Region 2	42	493–517	SU C terminus	0.0822
		43	505–529		0.3039
TM	Region 3	50	589–613	Ectodomain	0.4791
		51	601–625		0.0140†
	Region 4	56	660–685	Ectodomain	0.0053‡
	Region 5	61	721–746	Cytoplasmic domain	0.6818
		62	732–757		0.8188
	Region 6	71	841–865	Cytoplasmic domain	0.5237
		72	853–879		0.2451

*A *t*-test was performed by using data in Fig. 4 to determine differences in Ab reactivity between SIV239 infection and Δ5G infection.
†$P<0.05$; ‡$P<0.01$.

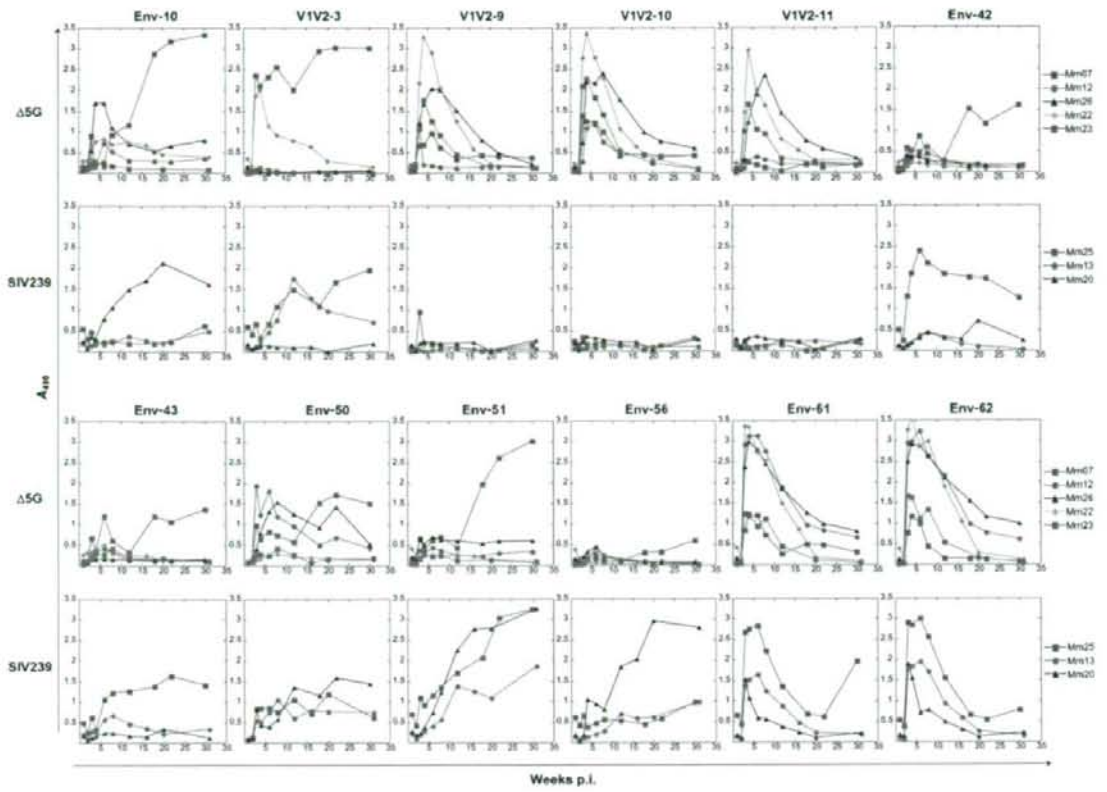

Fig. 6. Kinetics of peptide-specific Ab responses in Δ5G-infected and SIV239-infected animals. The kinetics of Ab reaction against peptides selected in the experiments shown in Figs 4 and 5 was determined as A_{490} using plasma diluted 1 : 100 in an ELISA.

Δ5G-specific, as no appreciable capture of SIV239 virion was detected with these samples. Furthermore, this activity was reduced to the level of control IgG (R374) after selective removal of IgG binding to V1V2-9, -10 and -11 peptides, suggesting that virion capture activity is associated with the Δ5G-specific linear epitope Ab (Fig. 7a). By contrast, IgG fractions from SIV239-infected animals collected at 3–4 weeks p.i. did not exhibit appreciable binding activity either to Δ5G virions or SIV239 virions (Fig. 7b). Thus, these results demonstrated that Δ5G infection elicited not only nAb after 8 weeks p.i., but also a much earlier humoral antiviral mechanism in the form of Δ5G-specific virion-binding Ab at 3–4 weeks p.i. in at least two monkeys (Mm07 and Mm22). To examine the relationship between the two antibody activities, we calculated the correlation of virion capture activity of IgG at 3 or 4 weeks p.i. with a peak nAb titre in Δ5G-infected animals (Fig. 2b) and found that this correlation was statistically significant ($r=1$, $P=0.0167$; Fig. 7c).

DISCUSSION

nAb response in Δ5G-infected animals

Glycosylation of viral spikes has long been recognized as an effective strategy to evade host (humoral) immune surveillance for several pathogens and for HIV/SIV in particular (Dowling *et al.*, 2007; Fournillier *et al.*, 2001; Haigwood & Stamatatos, 2003; Huso *et al.*, 1988; Reitter *et al.*, 1998). In support of these observations, the data presented here demonstrated that quintuple deglycosylation conferred live attenuated vaccine properties to an SIV239 mutant, Δ5G (Mori *et al.*, 2001); however, a cellular but not humoral response was detected as an immune correlate of the protection of Δ5G-infected animals against SIV239 challenge infection. Therefore, we assumed that the complete control of robust acute virus replication in Δ5G-infected animals beyond the initial cell-mediated control would be due to the development of rapid and effective nAbs. This study indicated that, whereas

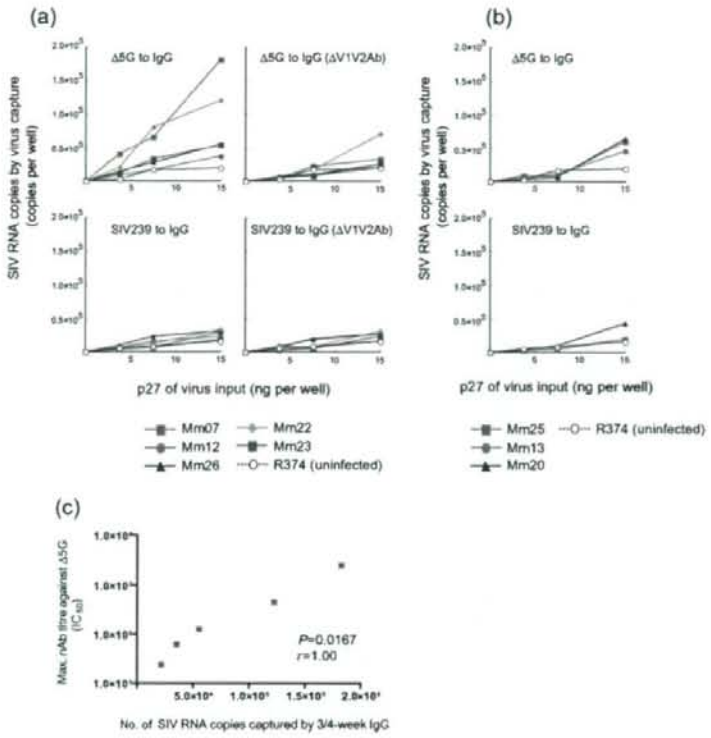

Fig. 7. Virion capture activity of IgG from Δ5G-infected and SIV239-infected animals. Virion capture activity of IgG from the plasma of infected animals at 3 or 4 weeks p.i. was determined by increased captured SIV RNA relative to input (3.75, 7.5 and 15 ng $p27^{gag}$) of Δ5G or SIV239. Plasma samples of Δ5G-infected animals (a) and SIV239-infected animals (b) were used for the assay. IgG (ΔV1V2Ab) indicates IgG depleted of Ab binding to V1V2-9, -10 or -11 peptide. R374 was an uninfected monkey. Correlation between virion capture activity at 3 or 4 weeks p.i. and peak nAb titre in Δ5G-infected animals (Fig. 2b) is shown (c).

Δ5G-infected animals clearly exhibited better nAb responses than SIV239-infected animals, the most stringent nAb assay, based on 90 % inhibition, provided evidence of nAb titres in only two of five Δ5G-infected animals and the appearance of these titres trailed the decline of acute viral loads by almost 4 weeks (Figs 1 and 2). Therefore, we concluded that, although deglycosylation did promote better development of nAbs in Δ5G-infection than SIV239 infection, it was still too late to control acute viraemia.

Zinkernagel and co-workers have categorized viruses into two types: 'acutely cytopathic viruses' and 'poorly or non-cytopathic viruses' (Hangartner *et al.*, 2006b). The former contains viruses such as vesicular stomatitis virus in mice and influenza virus in humans, whose control depends primarily on a rapid and potent nAb response. The latter comprises viruses such as lymphocytic choriomenigitis virus in mice, and hepatitis B and C viruses and HIV in humans, against which a nAb response is apparent only following the reduction of primary viraemia, and which establish persistent chronic infections. Accordingly, although the viral loads in Δ5G infection resembled 'acutely cytopathic virus' infections, the kinetics of nAbs still conformed to the 'non-cytopathic virus' category. As the difference in nAb response between the two types of virus is determined by their surface glycoproteins (Pinschewer *et al.*, 2004), this study suggests that the deglycosylation of Δ5G could not change this intrinsic property of SIV239.

Ab responses to Env peptides in Δ5G-infected animals

Aside from nAb, non-nAb responses to linear epitopes in V1/V2 were specifically induced by 3 weeks p.i. in all Δ5G-infected animals (Figs 4, 5 and 6). The heavy glycosylation of viral spikes clearly prevented access of B-cell receptors to the linear Ab epitopes located within limited regions of gp120 in SIV239, and the reduced glycosylation probably promoted better exposure of these linear epitopes in Δ5G (Fig. 4). Accordingly, the Δ5G-specific epitope in V1/V2 should be closely associated with the deglycosylation mutation at aa 171 in gp120 (Fig. 5). We speculate that this Ab induction might contribute to acute viral suppression in Δ5G infection because of the coincident decrease in peak viraemia (Figs 1 and 6). Non-neutralizing Abs can be divided into those that bind to the intact virion surface and debris-specific Ab. The former non-neutralizing Abs have occasional possibilities for antiviral activities such as antibody-dependent cell-mediated cytotoxicity and complement-mediated virus inactivation (Aasa-Chapman *et al.*, 2005; Ahmad & Menezes, 1996; Forthal *et al.*, 2001; Hangartner *et al.*, 2006a). In fact, readily detectable virion

capture Abs were induced in two of five Δ5G-infected animals (Fig. 7, Mm07 and Mm22). The importance of immediate-early suppression of SIV replication for the long-term containment of infection has been demonstrated by studies of post-exposure anti-retroviral therapy (Lifson *et al.*, 2000; Mori *et al.*, 2000). Thus, the early and complete control of viraemia in Δ5G-infected animals clearly suggests an antiviral mechanism(s) acting as early as 2–4 weeks p.i. Therefore, the early detection of IgG capable of virus capture in Δ5G-infected animals may provide mechanisms capable of contributing to undetectable viral load set points (Fig. 1b). The selective generation of such Ab directed to linear Env epitopes is expected.

Interestingly, deglycosylation in gp120 was also associated with a general reduction in the antigenicity of linear epitopes in gp41: the Ab response against the two epitopes that reside in the regions between the two heptad repeats (aa 601–625) and in the C-terminal heptad repeat (aa 660–685), respectively, was markedly reduced (Fig. 4, Table 1). The former corresponds to the highly conserved immunogenic epitope (Benichou *et al.*, 1993; Gnann *et al.*, 1987; Silvera *et al.*, 1994), and the latter corresponds to an epitope identified in the chronic phase of SIVmac251 infection (Silvera *et al.*, 1994) and corresponds to the nAb epitope of HIV-1 known as 2F5 (Muster *et al.*, 1993), although this linear epitope has not been associated with SIV neutralization (Caffrey *et al.*, 1998). Thus, these epitopes are probably exposed on the surface of viral spikes or their degraded fragments in most SIV and HIV-1 isolates with appropriate glycosylation and correct folding. We believe that the loss of glycosylation might induce a slight conformational change in the gp120 protein backbone, resulting in altered interaction of gp120 and gp41. In fact, the region encompassing the former epitope in gp41 was demonstrated to interact with gp120 (Cao *et al.*, 1993; Maerz *et al.*, 2001; York & Nunberg, 2004). As viral spikes determine virus properties such as viral receptor usage and cell tropism (Kolchinsky *et al.*, 2001; Puffer *et al.*, 2002), different cell populations might be infected in Δ5G-infected animals compared with SIV239 infection. More specifically, because of the distinct properties of the virus, vigorous Δ5G replication in the acute phase did not apparently impair immune function and thus established the control of chronic-phase infection and viral replication.

Host factors required for functional Ab responses against SIV infection

This study also demonstrated remarkable differences in humoral response with regard to nAb and virion capture Ab among Δ5G-infected animals. However, gp120-specific-binding Ab and the linear epitope-specific Ab were initially induced similarly in all animals. These findings imply that Abs measured by ELISA assay and Abs exhibiting antiviral activity are elicited by different pathways and that the properties associated with functional Abs depend largely on the host and underscore the importance of its genetic background. Rhesus macaques are present in various geographical locations within the Asian continent and are subdivided into many subspecies morphologically and genetically (Smith & McDonough, 2005). Some of the genetic differences among rhesus monkeys of different geographical origins, and especially those involving major histocompatibility complex (MHC) genotypes, probably influence the corresponding differences in immune responses, especially cellular response (Bontrop *et al.*, 1996; O'Connor *et al.*, 2003; Reimann *et al.*, 2005). Schmitz *et al.* (2005) reported that Mamu-A*01-positive rhesus monkeys elicited a significantly higher cellular response and lower nAb titres than those in Mamu-A*01-negative animals at the time of challenge infection of animals vaccinated with live attenuated SIV. They suggested that both humoral and cellular immune responses contributed to the protection against the challenge infection and that the relative contribution of each of the responses may be genetically determined. We observed a similar relationship between nAb and cellular responses among Δ5G-infected animals: two animals (Mm07 and Mm22) elicited a lower cellular response while the other three animals (Mm12, Mm23 and Mm26) elicited a higher cellular response (data not shown). Notably two animals exhibiting highly functional Ab (Mm07 and Mm22) were the offspring of seed animals imported from Laos, whilst the others (Mm12, Mm23 and Mm26) were of Burmese origin, suggesting the potential association of such different humoral and cellular responses with host genetic factors. In clinical studies, considerable concordance of adaptive cellular and humoral responses and HIV evolution in monozygotic twins, but not in brothers, infected with the same virus has been reported (Draenert *et al.*, 2006). HIV-1-exposed but uninfected status with significantly higher neutralizing IgA was linked to genotypes on chromosome 22 (Kanari *et al.*, 2005). In the mouse Friend leukemia virus model, MHC II alleles were determined as host genetic factors required for effective nAb response (Miyazawa *et al.*, 1992) and the host genetic factor was mapped to chromosome 15, which was associated with the clearance of viraemia by nAb (Hasenkrug *et al.*, 1995; Kanari *et al.*, 2005).

Taken together, we speculate that the functional humoral response is determined by host genetic properties similar to the cellular immune response. Thus, gaining knowledge of the genetic requirements for both humoral and cellular containment of viral infections will clearly be of primary importance for vaccine development and therapeutics against HIV and other infectious agents.

NOTE ADDED IN PROOF

A discrepancy in the SIV239-infected animals Mm13 and Mm20 was noted between the result shown in Fig. 2 and that in a previous report Mori *et al.*, 2001. The nAb

response against SIV239 in Mm20 was confirmed at multiple time points in the present study.

ACKNOWLEDGEMENTS

We thank Kayoko Ueda for excellent technical assistance and Marcelo Kuroda for critical reading of the manuscript. This study was conducted through the Cooperative Research Program in the Tsukuba Primate Research Center, National Institute of Biomedical Innovation, Japan. This work was supported by AIDS research grants from the Health Sciences Research Grants, from the Ministry of Health, Labour and Welfare in Japan, and from the Ministry of Education, Culture, Sports, Science and Technology in Japan.

REFERENCES

Aasa-Chapman, M. M., Holuigue, S., Aubin, K., Wong, M., Jones, N. A., Cornforth, D., Pellegrino, P., Newton, P., Williams, I. & other authors (2005). Detection of antibody-dependent complement-mediated inactivation of both autologous and heterologous virus in primary human immunodeficiency virus type 1 infection. *J Virol* **79**, 2823–2830.

Ahmad, A. & Menezes, J. (1996). Antibody-dependent cellular cytotoxicity in HIV infections. *FASEB J* **10**, 258–266.

Benichou, S., Venet, A., Beyer, C., Tiollais, P. & Madaule, P. (1993). Characterization of B-cell epitopes in the envelope glycoproteins of simian immunodeficiency virus. *Virology* **194**, 870–874.

Bontrop, R. E., Otting, N., Niphuis, H., Noort, R., Teeuwsen, V. & Heeney, J. L. (1996). The role of major histocompatibility complex polymorphisms on SIV infection in rhesus macaques. *Immunol Lett* **51**, 35–38.

Burns, D. P. & Desrosiers, R. C. (1991). Selection of genetic variants of simian immunodeficiency virus in persistently infected rhesus monkeys. *J Virol* **65**, 1843–1854.

Burton, D. R., Desrosiers, R. C., Doms, R. W., Koff, W. C., Kwong, P. D., Moore, J. P., Nabel, G. J., Sodroski, J., Wilson, I. A. & Wyatt, R. T. (2004). HIV vaccine design and the neutralizing antibody problem. *Nat Immunol* **5**, 233–236.

Caffrey, M., Cai, M., Kaufman, J., Stahl, S. J., Wingfield, P. T., Covell, D. G., Gronenborn, A. M. & Clore, G. M. (1998). Three-dimensional solution structure of the 44 kDa ectodomain of SIV gp41. *EMBO J* **17**, 4572–4584.

Cao, J., Bergeron, L., Helseth, E., Thali, M., Repke, H. & Sodroski, J. (1993). Effects of amino acid changes in the extracellular domain of the human immunodeficiency virus type 1 gp41 envelope glycoprotein. *J Virol* **67**, 2747–2755.

Chackerian, B., Rudensey, L. M. & Overbaugh, J. (1997). Specific *N*-linked and *O*-linked glycosylation modifications in the envelope V1 domain of simian immunodeficiency virus variants that evolve in the host alter recognition by neutralizing antibodies. *J Virol* **71**, 7719–7727.

Chen, B., Vogan, E. M., Gong, H., Skehel, J. J., Wiley, D. C. & Harrison, S. C. (2005). Structure of an unliganded simian immunodeficiency virus gp120 core. *Nature* **433**, 834–841.

Cheng-Mayer, C., Brown, A., Harouse, J., Luciw, P. A. & Mayer, A. J. (1999). Selection for neutralization resistance of the simian/human immunodeficiency virus $SHIV_{SF33A}$ variant in vivo by virtue of sequence changes in the extracellular envelope glycoprotein that modify *N*-linked glycosylation. *J Virol* **73**, 5294–5300.

Choi, W. S., Collignon, C., Thiriart, C., Burns, D. P., Stott, E. J., Kent, K. A. & Desrosiers, R. C. (1994). Effects of natural sequence variation on recognition by monoclonal antibodies neutralize simian immunodeficiency virus infectivity. *J Virol* **68**, 5395–5402.

Dowling, W., Thompson, E., Badger, C., Mellquist, J. L., Garrison, A. R., Smith, J. M., Paragas, J., Hogan, R. J. & Schmaljohn, C. (2007). Influences of glycosylation on antigenicity, immunogenicity, and protective efficacy of Ebola virus GP DNA vaccines. *J Virol* **81**, 1821–1837.

Draenert, R., Allen, T. M., Liu, Y., Wrin, T., Chappey, C., Verrill, C. L., Sirera, G., Eldridge, R. L., Lahaie, M. P. & other authors (2006). Constraints on HIV-1 evolution and immunodominance revealed in monozygotic adult twins infected with the same virus. *J Exp Med* **203**, 529–539.

Eberle, J., Loussert-Ajaka, I., Brust, S., Zekeng, L., Hauser, P. H., Kaptue, L., Knapp, S., Damond, F., Saragosti, S. & other authors (1997). Diversity of the immunodominant epitope of gp41 of HIV-1 subtype O and its validity for antibody detection. *J Virol Methods* **67**, 85–91.

Forthal, D. N., Landucci, G. & Keenan, B. (2001). Relationship between antibody-dependent cellular cytotoxicity, plasma HIV type 1 RNA, and $CD4^+$ lymphocyte count. *AIDS Res Hum Retroviruses* **17**, 553–561.

Fournillier, A., Wychowski, C., Boucreux, D., Baumert, T. F., Meunier, J. C., Jacobs, D., Muguet, S., Depla, E. & Inchauspe, G. (2001). Induction of hepatitis C virus E1 envelope protein-specific immune response can be enhanced by mutation of *N*-glycosylation sites. *J Virol* **75**, 12088–12097.

Gnann, J. W., Jr, Nelson, J. A. & Oldstone, M. B. (1987). Fine mapping of an immunodominant domain in the transmembrane glycoprotein of human immunodeficiency virus. *J Virol* **61**, 2639–2641.

Haigwood, N. L. & Stamatatos, L. (2003). Role of neutralizing antibodies in HIV infection. *AIDS* **17** (Suppl. 4), S67–S71.

Hangartner, L., Zellweger, R. M., Giobbi, M., Weber, J., Eschli, B., McCoy, K. D., Harris, N., Recher, M., Zinkernagel, R. M. & Hengartner, H. (2006a). Nonneutralizing antibodies binding to the surface glycoprotein of lymphocytic choriomeningitis virus reduce early virus spread. *J Exp Med* **203**, 2033–2042.

Hangartner, L., Zinkernagel, R. M. & Hengartner, H. (2006b). Antiviral antibody responses: the two extremes of a wide spectrum. *Nat Rev Immunol* **6**, 231–243.

Hasenkrug, K. J., Valenzuela, A., Letts, V. A., Nishio, J., Chesebro, B. & Frankel, W. N. (1995). Chromosome mapping of *Rfv3*, a host resistance gene to Friend murine retrovirus. *J Virol* **69**, 2617–2620.

Hofmann-Lehmann, R., Swenerton, R. K., Liska, V., Leutenegger, C. M., Lutz, H., McClure, H. M. & Ruprecht, R. M. (2000). Sensitive and robust one-tube real-time reverse transcriptase-polymerase chain reaction to quantify SIV RNA load: comparison of one- versus two-enzyme systems. *AIDS Res Hum Retroviruses* **16**, 1247–1257.

Huso, D. L., Narayan, O. & Hart, G. W. (1988). Sialic acids on the surface of caprine arthritis-encephalitis virus define the biological properties of the virus. *J Virol* **62**, 1974–1980.

Johnson, W. E., Sanford, H., Schwall, L., Burton, D. R., Parren, P. W., Robinson, J. E. & Desrosiers, R. C. (2003). Assorted mutations in the envelope gene of simian immunodeficiency virus lead to loss of neutralization resistance against antibodies representing a broad spectrum of specificities. *J Virol* **77**, 9993–10003.

Kanari, Y., Clerici, M., Abe, H., Kawabata, H., Trabattoni, D., Caputo, S. L., Mazzotta, F., Fujisawa, H., Niwa, A. & other authors (2005). Genotypes at chromosome 22q12–13 are associated with HIV-1-exposed but uninfected status in Italians. *AIDS* **19**, 1015–1024.

Kent, K. A., Rud, E., Corcoran, T., Powell, C., Thiriart, C., Collignon, C. & Stott, E. J. (1992). Identification of two neutralizing and 8 non-neutralizing epitopes on simian immunodeficiency virus envelope

using monoclonal antibodies. *AIDS Res Hum Retroviruses* **8**, 1147–1151.

Kolchinsky, P., Kiprilov, E., Bartley, P., Rubinstein, R. & Sodroski, J. (2001). Loss of a single *N*-linked glycan allows CD4-independent human immunodeficiency virus type 1 infection by altering the position of the gp120 V1/V2 variable loops. *J Virol* **75**, 3435–3443.

Leonard, C. K., Spellman, M. W., Riddle, L., Harris, R. J., Thomas, J. N. & Gregory, T. J. (1990). Assignment of intrachain disulfide bonds and characterization of potential glycosylation sites of the type 1 recombinant human immunodeficiency virus envelope glycoprotein (gp120) expressed in Chinese hamster ovary cells. *J Biol Chem* **265**, 10373–10382.

Lifson, J. D., Rossio, J. L., Arnaout, R., Li, L., Parks, T. L., Schneider, D. K., Kiser, R. F., Coalter, V. J., Walsh, G. & other authors (2000). Containment of simian immunodeficiency virus infection: cellular immune responses and protection from rechallenge following transient postinoculation antiretroviral treatment. *J Virol* **74**, 2584–2593.

Liu, J., Wang, S., Hoxie, J. A., LaBranche, C. C. & Lu, M. (2002). Mutations that destabilize the gp41 core are determinants for stabilizing the simian immunodeficiency virus-CPmac envelope glycoprotein complex. *J Biol Chem* **277**, 12891–12900.

Maerz, A. L., Drummer, H. E., Wilson, K. A. & Poumbourios, P. (2001). Functional analysis of the disulfide-bonded loop/chain reversal region of human immunodeficiency virus type 1 gp41 reveals a critical role in gp120-gp41 association. *J Virol* **75**, 6635–6644.

Means, R. E., Greenough, T. & Desrosiers, R. C. (1997). Neutralization sensitivity of cell culture-passaged simian immunodeficiency virus. *J Virol* **71**, 7895–7902.

Miyazawa, M., Nishio, J., Wehrly, K. & Chesebro, B. (1992). Influence of MHC genes on spontaneous recovery from Friend retrovirus-induced leukemia. *J Immunol* **148**, 644–647.

Mori, K., Yasutomi, Y., Sawada, S., Villinger, F., Sugama, K., Rosenwith, B., Heeney, J. L., Uberla, K., Yamazaki, S. & other authors (2000). Suppression of acute viremia by short-term postexposure prophylaxis of simian/human immunodeficiency virus SHIV-RT-infected monkeys with a novel reverse transcriptase inhibitor (GW420867) allows for development of potent antiviral immune responses resulting in efficient containment of infection. *J Virol* **74**, 5747–5753.

Mori, K., Yasutomi, Y., Ohgimoto, S., Nakasone, T., Takamura, S., Shioda, T. & Nagai, Y. (2001). Quintuple deglycosylation mutant of simian immunodeficiency virus SIVmac239 in rhesus macaques: robust primary replication, tightly contained chronic infection, and elicitation of potent immunity against the parental wild-type strain. *J Virol* **75**, 4023–4028.

Mori, K., Sugimoto, C., Ohgimoto, S., Nakayama, E. E., Shioda, T., Kusagawa, S., Takebe, Y., Kano, M., Matano, T. & other authors (2005). Influence of glycosylation on the efficacy of an Env-based vaccine against simian immunodeficiency virus SIVmac239 in a macaque AIDS model. *J Virol* **79**, 10386–10396.

Muster, T., Steindl, F., Purtscher, M., Trkola, A., Klima, A., Himmler, G., Ruker, F. & Katinger, H. (1993). A conserved neutralizing epitope on gp41 of human immunodeficiency virus type 1. *J Virol* **67**, 6642–6647.

Nishimura, Y., Igarashi, T., Haigwood, N., Sadjadpour, R., Plishka, R. J., Buckler-White, A., Shibata, R. & Martin, M. A. (2002). Determination of a statistically valid neutralization titer in plasma that confers protection against simian-human immunodeficiency virus challenge following passive transfer of high-titered neutralizing antibodies. *J Virol* **76**, 2123–2130.

Nyambi, P. N., Gorny, M. K., Bastiani, L., van der Groen, G., Williams, C. & Zolla-Pazner, S. (1998). Mapping of epitopes exposed on intact human immunodeficiency virus type 1 (HIV-1) virions: a new strategy for studying the immunologic relatedness of HIV-1. *J Virol* **72**, 9384–9391.

O'Connor, D. H., Mothe, B. R., Weinfurter, J. T., Fuenger, S., Rehrauer, W. M., Jing, P., Rudersdorf, R. R., Liebl, M. E., Krebs, K. & other authors (2003). Major histocompatibility complex class I alleles associated with slow simian immunodeficiency virus disease progression bind epitopes recognized by dominant acute-phase cytotoxic-T-lymphocyte responses. *J Virol* **77**, 9029–9040.

Ohgimoto, S., Shioda, T., Mori, K., Nakayama, E. E., Hu, H. & Nagai, Y. (1998). Location-specific, unequal contribution of the *N* glycans in simian immunodeficiency virus gp120 to viral infectivity and removal of multiple glycans without disturbing infectivity. *J Virol* **72**, 8365–8370.

Pinschewer, D. D., Perez, M., Jeetendra, E., Bachi, T., Horvath, E., Hengartner, H., Whitt, M. A., de la Torre, J. C. & Zinkernagel, R. M. (2004). Kinetics of protective antibodies are determined by the viral surface antigen. *J Clin Invest* **114**, 988–993.

Puffer, B. A., Pohlmann, S., Edinger, A. L., Carlin, D., Sanchez, M. D., Reitter, J., Watry, D. D., Fox, H. S., Desrosiers, R. C. & Doms, R. W. (2002). CD4 independence of simian immunodeficiency virus Envs is associated with macrophage tropism, neutralization sensitivity, and attenuated pathogenicity. *J Virol* **76**, 2595–2605.

Regier, D. A. & Desrosiers, R. C. (1990). The complete nucleotide sequence of a pathogenic molecular clone of simian immunodeficiency virus. *AIDS Res Hum Retroviruses* **6**, 1221–1231.

Reimann, K. A., Parker, R. A., Seaman, M. S., Beaudry, K., Beddall, M., Peterson, L., Williams, K. C., Veazey, R. S., Montefiori, D. C. & other authors (2005). Pathogenicity of simian-human immunodeficiency virus SHIV-89.6P and SIVmac is attenuated in cynomolgus macaques and associated with early T-lymphocyte responses. *J Virol* **79**, 8878–8885.

Reitter, J. N., Means, R. E. & Desrosiers, R. C. (1998). A role for carbohydrates in immune evasion in AIDS. *Nat Med* **4**, 679–684.

Schmitz, J. E., Johnson, R. P., McClure, H. M., Manson, K. H., Wyand, M. S., Kuroda, M. J., Lifton, M. A., Khunkhun, R. S., McEvers, K. J. & other authors (2005). Effect of $CD8^+$ lymphocyte depletion on virus containment after simian immunodeficiency virus SIVmac251 challenge of live attenuated SIVmac239Δ3-vaccinated rhesus macaques. *J Virol* **79**, 8131–8141.

Silvera, P., Flanagan, B., Kent, K., Rud, E., Powell, C., Corcoran, T., Bruck, C., Thiriart, C., Haigwood, N. L. & Stott, E. J. (1994). Fine analysis of humoral antibody response to envelope glycoprotein of SIV in infected and vaccinated macaques. *AIDS Res Hum Retroviruses* **10**, 1295–1304.

Smith, D. G. & McDonough, J. (2005). Mitochondrial DNA variation in Chinese and Indian rhesus macaques (*Macaca mulatta*). *Am J Primatol* **65**, 1–25.

Wei, X., Decker, J. M., Wang, S., Hui, H., Kappes, J. C., Wu, X., Salazar-Gonzalez, J. F., Salazar, M. G., Kilby, J. M. & other authors (2003). Antibody neutralization and escape by HIV-1. *Nature* **422**, 307–312.

Wyatt, R. & Sodroski, J. (1998). The HIV-1 envelope glycoproteins: fusogens, antigens, and immunogens. *Science* **280**, 1884–1888.

Wyatt, R., Kwong, P. D., Desjardins, E., Sweet, R. W., Robinson, J., Hendrickson, W. A. & Sodroski, J. G. (1998). The antigenic structure of the HIV gp120 envelope glycoprotein. *Nature* **393**, 705–711.

York, J. & Nunberg, J. H. (2004). Role of hydrophobic residues in the central ectodomain of gp41 in maintaining the association between human immunodeficiency virus type 1 envelope glycoprotein subunits gp120 and gp41. *J Virol* **78**, 4921–4926.

Yu, D., Shioda, T., Kato, A., Hasan, M. K., Sakai, Y. & Nagai, Y. (1997). Sendai virus-based expression of HIV-1 gp120: reinforcement by the V(−) version. *Genes Cells* **2**, 457–466.

Zhang, M., Gaschen, B., Blay, W., Foley, B., Haigwood, N., Kuiken, C. & Korber, B. (2004). Tracking global patterns of *N*-linked glycosylation site variation in highly variable viral glycoproteins: HIV, SIV, and HCV envelopes and influenza hemagglutinin. *Glycobiology* **14**, 1229–1246.

Zolla-Pazner, S. (2004). Identifying epitopes of HIV-1 that induce protective antibodies. *Nat Rev Immunol* **4**, 199–210.

Neuropathology 2008 doi:10.1111/j.1440-1789.2008.00929.x

Original Article

Expression of proinflammatory cytokines and its relationship with virus infection in the brain of macaques inoculated with macrophage-tropic simian immunodeficiency virus

Hui Qin Xing,[1] Takashi Moritoyo,[1] Kazuyasu Mori,[2,3] Chie Sugimoto,[2,3] Fumiko Ono[4] and Shuji Izumo[1]

[1]Division of Molecular Pathology, Center for Chronic Viral Diseases, Graduate School of Medical and Dental Sciences, Kagoshima University, Kagoshima, [2]AIDS Research Center, National Institute of Infectious Diseases, Shinjuku-ku, Tokyo, [3]Tsukuba Primate Research Center, National Institute of Biomedical Innovation, and [4]Corporation for Production and Research of Laboratory Primates, Ibaraki, Japan

The pathogenesis of acquired immunodeficiency syndrome dementia complex (ADC) is still poorly understood. Many studies suggest that proinflammatory cytokines such as IL-1β and TNF-α released by microglia/macrophages or astrocytes play a role in CNS injury. A microscopic finding of a microglial nodule with multinucleated giant cells (MNGCs) is a histopathologic hallmark of ADC and named HIV encephalitis. However, in vivo expression of these cytokines in this microenvironment of HIV encephalitis is not yet clarified. One of the main reasons is complexities of brain pathology in patients who have died from terminal AIDS. In this study, we infected two macaques with macrophage-tropic Simian immunodeficiency virus SIV239env/MERT and examined expression of TNF-α and IL-1β in inflammatory lesions with MNGCs and its relation to virus-infected cells using immunohistochemistry. One macaque showed typical inflammatory lesions with MNGCs in the frontal white matter. Small microglial nodules were also detected in the basal ganglia and the spinal cord. SIVenv positive cells were detected mainly in inflammatory lesions, and seemed to be microglia/macrophages and MNGCs based on their morphology. Expression of IL-1β and TNF-α were detected in the inflammatory lesions with MNGCs, and these positive cells were found to be negative for SIVenv by double-labeling immunohistochemistry or immunohistochemistry of serial sections. There were a few TNF-α positive cells and almost no IL-1β positive cells in the area other than inflammatory lesions. Another macaque showed scattered CD3+ cells and CD68+ cells in the perivascular regions of the white matter. SIVenv and TNF-α was demonstrated in a few perivascular macrophages. These findings indicate that virus-infected microglia/macrophages do not always express IL-1β and TNF-α, which suggests an indirect role of HIV-1-infected cells in cytokine-mediated pathogenesis of ADC. Our macaque model for human ADC may be useful for better understanding of its pathogenesis.

Key words: cytokines, HIV encephalitis, macaque model, macrophage-tropic, simian immunodeficiency virus.

INTRODUCTION

Human immunodeficiency virus-1 (HIV-1) can induce a clinical triad of progressive cognitive decline, motor dysfunction, and behavioral abnormalities named acquired immunodeficiency syndrome dementia complex (ADC). Although the introduction of highly active anti-retroviral therapy (HAART) has been successful to reduce progression of acquired immunodeficiency syndrome (AIDS), controversial results have been reported that the prevalence of dementia may eventually increase, corresponding to a longer life span of people with HIV-1 infection.[1–3]

Acquired immunodeficiency syndrome dementia complex is histopathologically identified by diffuse and

Correspondence: Hui Qin Xing, MD, PhD, Division of Molecular Pathology, Center for Chronic Viral Diseases, Graduate School of Medical and Dental Sciences, Kagoshima University, 8-35-1 Sakuragaoka, Kagoshima 890-8544, Japan. Email: xhqw63@hotmail.com

Received 27 December 2007; revised and accepted 26 March 2008

nodular microgliosis with formation of multinucleated giant cells (MNGCs) in the white mater of the brain and is termed HIV encephalitis.[4,5] Myelin pallor[6] and axonal damage[7-9] with abundant HIV-infected macrophages and microglial cells have been demonstrated in the white mater.[5,10] Many studies suggest proinflammatory cytokines such as IL-1β and TNF-α released by microglia and macrophages which play a role in CNS injury.[11,12] On the other hand, infection of astrocytes may also occur with limited virus replication,[13] and astrocytes could cause CNS injury by secreting cytokines.[14-17] These observations suggest a role of proinflammatory cytokines in ADC. However, in vivo expression of these cytokines in the microenvironment of HIV encephalitis, microglial nodules with MNGCs, the histopathologic hallmark of ADC, is not yet clarified. One of the main reasons is presumed to be the complexities of brain pathology in patients who have died from terminal AIDS.

Simian immunodeficiency virus (SIV) infection of macaques has been shown to recapitulate key features of HIV infection of the human CNS, including the development of encephalitis with characteristic histopathological changes and psychomotor impairment.[18,19] Our previous study demonstrated that a macrophage-tropic SIV, SIV239env/MERT, caused typical microglial nodules with MNGCs without development of AIDS. Using this animal model of HIV-1 encephalitis, we explored which cell types expressed TNF-α and IL-1β and whether it is related to viral infection in the microenvironment of SIV encephalitis.

MATERIALS AND METHODS

Virus and animal

SIV239env/MERT is a macrophage-tropic virus the pathogenic properties of which have been previously described. This virus comprises four amino acid substitutions in the env of SIVmac239 backbone, and replicates as efficiently as the highly macrophage-tropic virus SIVmac316 in the alveolar macrophages.[20]

The rhesus macaques were screened and found to be seronegative for SIV, STLV, B virus, and type D retroviruses. Two macaques, #531 and #626, were infected intravenously with 100 TCID50 of SIV239env/MERT. Three uninfected macaques were used as controls. The animals were housed in individual cages and maintained according to the rules and guidelines of the National Institute for Infectious Diseases (NIID) for experimental animal welfare.

CD4+ cell count and viral RNA load

CD4+ cell counts were performed in peripheral blood specimens at the time of autopsy. To measure the level of virus replication in the periphery, viral RNA was quantified in plasma at autopsy. Viral RNA in the plasma of inoculated macaques was measured by real-time RT_PCR.

Histopathological examination

Routine histopathological methods applied are described elsewhere.[21] In brief, coronal sections of the brain and spinal cord were embedded in paraffin. For routine light microscopy, the paraffin sections were stained with HE and KB.

We used EnVision system (Dako, Carpinteria, CA, US) for immunohistochemistry. The following antibodies were used as the first antibodies: a mouse monoclonal antibody (mAb) anti-human TNF-α (1:400, abcam K. K., Tokyo, Japan), a rabbit polyclonal antibody IL-1β (1:200, Santa Cruz Biotechnology, Santa Cruz, CA, US), a mAb anti-GFAP (1:100; Chemicon International, Temecula, CA, US), a rabbit anti-human CD3 (1:50; Dako, Glostrup, Denmark), a mAb anti-human macrophage CD68 (KP1; 1:50; Dako), a rabbit anti-Iba1 antibody (1:500, Wako Pure Chemical Industries, Osaka, Japan), and a mAb anti–SIV envelope gp160/gp32, KK41 (1:50; National Institute for Biological Standards and Control, Herts, UK). Immunoreactivity was visualized using either diaminobenzidine/peroxidase or 3-amino-9-ethylcarbazole (Dako, Carpinteria, CA, US) substrate–chromogen system (Dako). Light counterstaining was done with hematoxylin. For the SIV envelope gp160/gp32 immunostaning, a lymph node section from an SIV-infected rhesus macaque was used as a positive control. In the same way, for the TNF-α and IL-1β immunostaining, a tonsil section was used as a positive control.

Double-label immunohistochemistry

We performed double-label immunohistochemistry for IL-1β and SIVKK41 using the same section to examine the expressions of IL-1β correlating with the SIVenvgp160/gp32- positive cells. This entailed performing immunohistochemistry for IL-1β, followed by immunohistochemistry for SIVKK41. Double labeling was performed using AEC/peroxidase followed by Vector blue/alkaline phosphatase.

RESULTS

Clinical manifestation

Macaque #531 showed very slow progression of clinical course. A CD4+ cell count remained moderately decreased, 270/μL, even long after infection, and was sacrificed for autopsy 154 weeks after infection. Plasma viral load was relatively high, 277 800 copies/mL, at autopsy. Macaque #626 also showed also progression of clinical

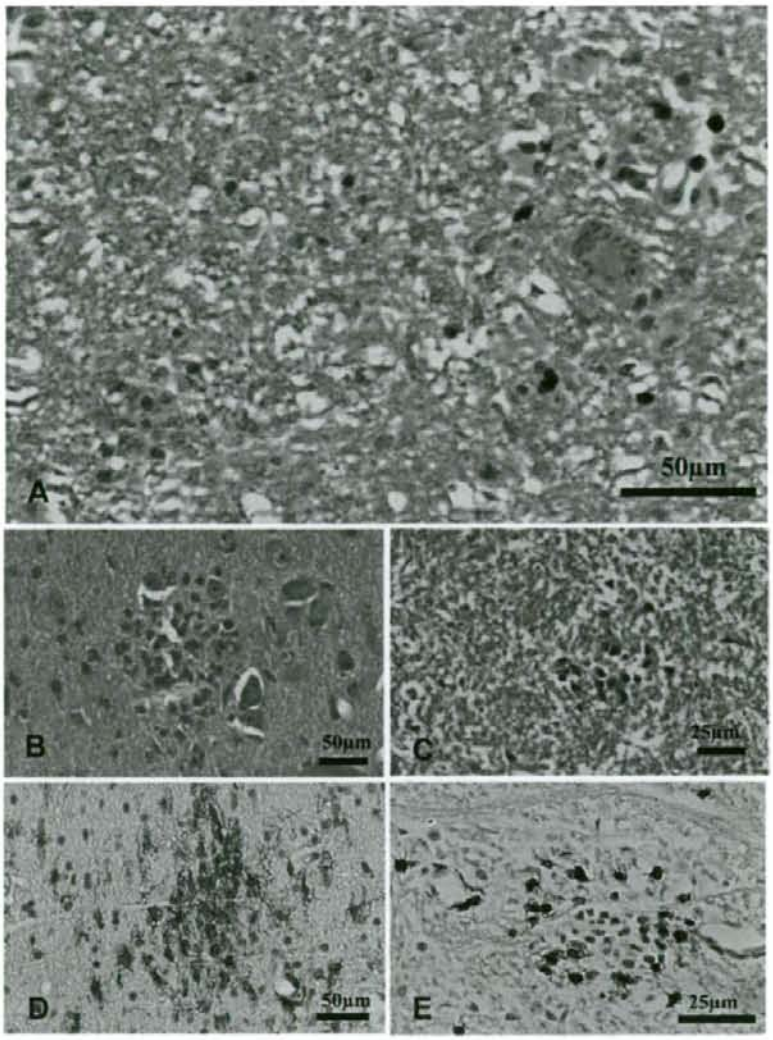

Fig. 1 Histopathological findings of the brain in macaque #531. A typical inflammatory lesion with microglial nodule with multinucleated giant cells (MNGCs) in the frontal white matter (A). Small microglial nodules seen in the basal ganglia (B), and the spinal cord (C). Microglial nodules were mainly composed of microglia/macrophages (D), and CD3+ T-cells (E). A, B, and C: HE; D: CD68; E: CD3. A: frontal white matter, B and D: basal ganglia, C and E: spinal cord.

course. CD4+ cell count remained moderately decreased, 220/μL, even long after infection. It was sacrificed for autopsy 218 weeks after infection. Plasma viral load remained low, 1000 copies/mL, at autopsy. These two macaques did not show obvious neurological symptoms or behavior abnormality.

Histopathological findings of the brain and lymph nodes

Macaque #531 showed a pathological hallmark of AIDS encephalopathy such as typical inflammatory lesions with MNGCs in the frontal white matter, (Fig. 1A). To a lesser extent, microglial nodules were also detected in the basal ganglia and spinal cord (Fig. 1B–C). Microglial nodules were mainly composed of microglia/macrophages (Fig. 1D), and CD3+ T-cells were scattered in the surrounding areas (Fig. 1E). Astrocytic gliosis was not accentuated in the areas of microglia nodules. On the other hand, no abnormality was observed in the cerebral cortex and cerebellum. Another macaque, #626, showed scattered CD3+ cells and CD68+ cells in the perivascular regions of the white matter and the meninges. However, microglial nodules with MNGCs could not be found. No other pathologic abnormality was found in the brain.

Virus-infected cells were detected by the immunostaining of the SIVenvgp160/gp32. In macaque #531, positive cells were detected mainly in inflammatory lesions

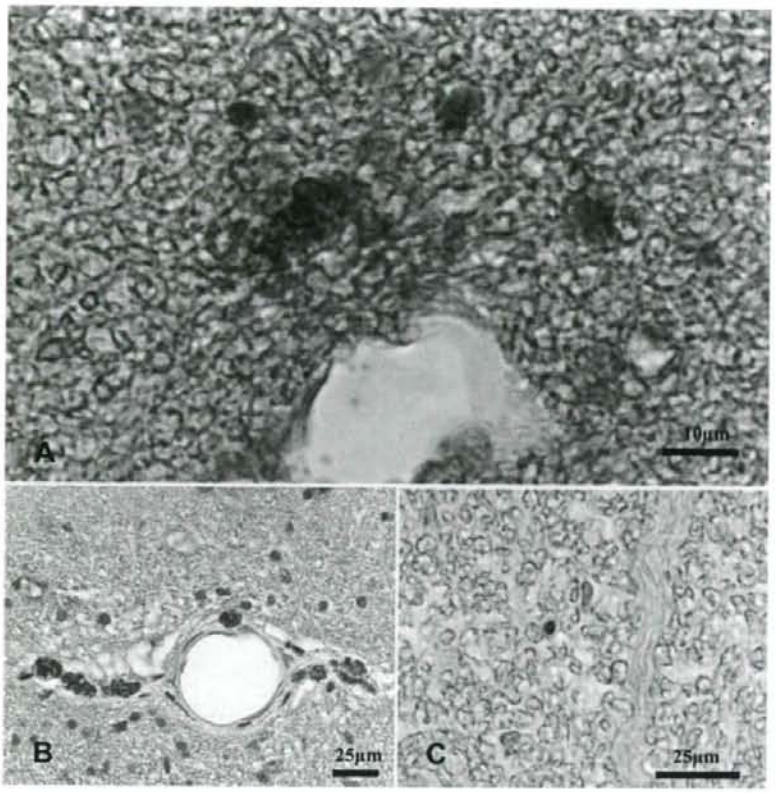

Fig. 2 Expression of a simian immunodeficiency virus (SIV) envelope protein by the immunostaining of SIVenvgp160/gp32 in macaque #531. SIV envelope protein is demonstrated in an inflammatory lesion in the frontal white matter (A), some perivascular macrophages in the basal ganglia (B), and a few in the spinal cord (C).

(Figs 2A,4B), and seemed to be microglia/macrophages and MNGCs based on their morphology. Some perivascular macrophages were also positive in basal ganglia (Fig. 2B). We also detected a few positive cells in the cerebellum and the spinal cord (Fig. 2C) as well as meningeal mononuclear cells. In another macaque, #626, SIVenvgp160/gp32 positive cells were limited to a few perivascular and meningeal mononuclear cells.

The lymph nodes of two virus-infected animals showed hyperplasia of follicles and their germinal centers showed irregular shapes. Decrease of CD3+ T-cells in the paracortical region was not evident.

All control macaques showed no abnormality in both brains and lymph nodes.

The expressions of TNF-α and IL-1β in inflammatory lesions

Since macaque #531 showed typical inflammatory lesions with MNGCs, we further examined expression of proinflammatory cytokines by immunohistochemistry. IL-1β-positive cells showed intracytoplasmic labeling. Positive cells were detected only in inflammatory lesions with MNGCs of the frontal white matter, that is to say, we could not detect IL-1β-positive cells in the parenchyma of basal ganglia as well as in the spinal cord. In order to investigate the relation between expression of IL-1β and virus infection, we performed double-label immunohistochemistry for IL-1β and SIVenvgp160/gp32. Interestingly, the IL-1β positive cells were found around the SIVenvgp160/gp32-positive cells, but not SIVenvgp160/gp32-positive cells (Fig. 3). The brain parenchyma of macaque #626 did not showed any IL-1β-positive cells.

TNF-α was also labeled as cytoplasmic staining. Positive cells were detected in some mononuclear cells of inflammatory lesions in the frontal white matter and basal ganglia, as well as a few perivascular macrophages. We could not detect TNF-α-positive cells in the spinal cord. TNF-α-positive cells seemed to be SIVenvgp160/gp32-negative cells in comparison with distribution of SIVenvgp160/gp32-positive cells stained using a serial section (Fig. 4). In macaque #626, a few TNF-α-positive cells were detected in perivascular and meningeal mononuclear cells.

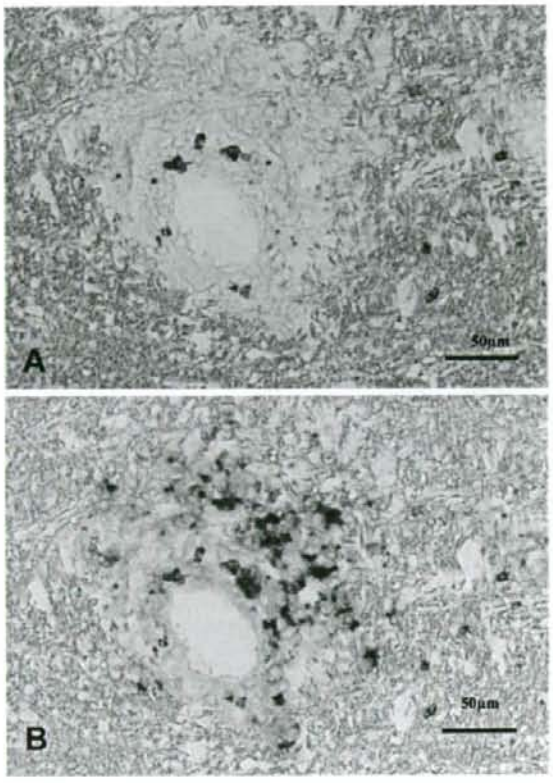

Fig. 3 Expression of IL-1β and SIVenvgp160/gp32 in an inflammatory lesion with microglial nodule with multinucleated giant cells (MNGCs). (A) IL-1β-positive cells are detected only in an inflammatory lesion with MNGCs seen in the frontal white matter of macaque #531. (B) IL-1β positive cells were found around the SIVenvgp160/gp32-positive cells but not SIVenvgp160/gp32-positive cells demonstrated by double-labeling immunohistochemistry performed using the same section of (A). A: anti-IL-1β; B: double-label immunohistochemistry for IL-1β (red) and SIVenvgp160/ gp32 (dark blue).

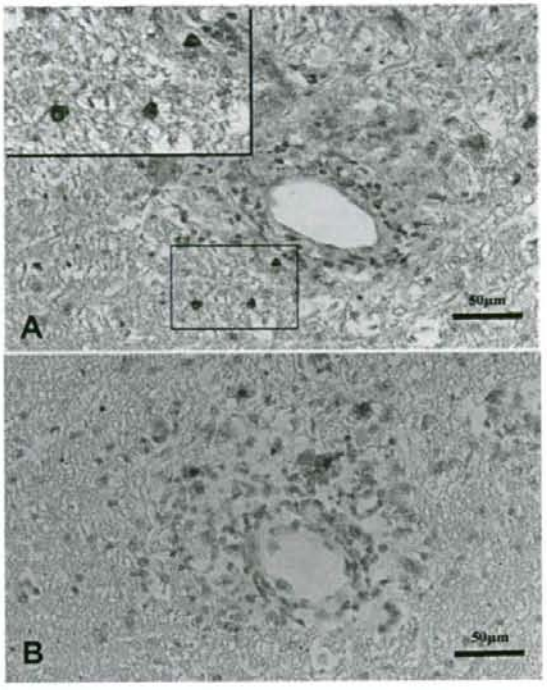

Fig. 4 Expression of TNF-α and SIVenvgp160/gp32 in an inflammatory lesion with microglial nodule with multinucleated giant cells (MNGCs). (A): TNF-α-positive cells are detected in mononuclear cells of an inflammatory lesion with MNGCs seen in the frontal white matter of macaque #531. (B): Distribution of SIVenvgp160/gp32-positive cells differs from that of TNF-α-positive cells demonstrated by SIVenvgp160/gp32 immunohistochemistry of serial section. A: anti-TNF-α, B: anti-SIVenvgp160/gp32.

DISCUSSION

Cytokines such as TNF-α and IL-1β may have toxic effects on CNS cells and have been postulated to contribute to the pathogenesis of the neurological complications of human immunodeficiency virus (HIV) infection.[22] However many of such studies were done by in vitro experiments; exposure of macrophages and microglia to either gp120 or Tat resulted in up-regulation of TNF-α expression,[23,24] and exposure of microglia to gp120 resulted in the production of IL-1β.[25,26] In contrast, there are only a few reports which demonstrated proinflammatory cytokines in the AIDS brain tissues directly in vivo. Tyor *et al.*[11] reported that there were significant increases in IL-1β and TNF-α in HIV-positive patients compared with HIV-negative brains, but no correlation was found between levels of cytokines and the presence or absence of CNS disease among HIV-positive individuals. In addition, in vivo expression of these cytokines in the microenvironment of HIV encephalitis, microglial nodules with MNGCs, was not demonstrated in their study. Zhao *et al.*[27] reported that IL-1β was expressed at high levels in areas of microglial nodules in HIV encephalitis. Because some MNGCs were positive for IL-1β in their report, they suggested that IL-1β was induced by HIV-1 infection.

In our present study, expression of IL-1β and TNF-α were detected in the inflammatory lesions with MNGCs, and these positive cells were found to be negative for SIVenvgp160/gp32. There were a few TNF-α positive cells and almost no IL-1β positive cells in the area other than inflammatory lesions including microglial nodules. Our findings indicate that virus-infected microglia/macrophages do not always express IL-1β and TNF-α. The

findings seen in macaque #531 might indicate a limited role of IL-1β and TNF-α in the very early stage of ADC. In order to understand a precise role of proinflammatory cytokines in ADC, further studies are required focusing on origin or nature of the cells expressing proinflammatory cytokines.

The differences between previous reports[22,27] and our present data about in vivo expression of cytokines might be explained by complexities of brain pathology in patients who have died from terminal AIDS. Human autopsies were usually performed in the advanced stages of AIDS. In such conditions, the brains may contain a variety of pathologic conditions other than HIV encephalitis such as diffuse poliodystrophy, another pathologic event of ADC, many kinds of opportunistic infections and tumors, and/or effects of anti-viral agents. Our macaque #531 with typical pathologic findings of SIV encephalitis was not in the stage of AIDS, and opportunistic diseases or diffuse poliodystrophy were not observed. We can also exclude the effects of chemotherapy.

In the present study, macaque #531 with typical SIV encephalitis did not show obvious neurological symptoms or behavior abnormality. This reminded us of a previous report in which the brains of asymptomatic HIV-1-positive individuals who died accidentally revealed HIV-1 infection and inflammatory response in the cerebral white matter.[28] These observations indicate that histopathologic findings of HIV encephalitis might be subclinical in many individuals infected with HIV-1. Another macaque (#626) did not show microglial nodules with MNGCs. The plasma viral load of this animal was much lower than that of macaque #531. This suggested that presence or absence of HIV encephalitis might simply depend on the value of plasma viral load.

Our macaque infected with SIV239env/MERT induced typical microglial nodules with MNGCs as a model of HIV encephalitis, and this macaque model may be useful for the better understanding of HIV encephalitis pathogenesis.

ACKNOWLEDGMENTS

This work was supported by AIDS research grants from the Health Sciences Research Grants, from the Ministry of Health, Labour, and Welfare in Japan. The authors thank Ms. Tomita Y, of Kagoshima University for excellent technical assistance.

REFERENCES

1. Jellinger KA, Setinek U, Drlicek M, Bohm G, Steurer A, Lintner F. Neuropathology and general autopsy findings in AIDS during the last 15 years. *Acta Neuropathol* 2000; **100**: 213–220.
2. Dore GJ, Correll PK, Li Y, Kaldor JM, Cooper DA, Brew BJ. Changes to AIDS dementia complex in the era of highly active antiretroviral therapy. *AIDS* 1999; **13**: 1249–1253.
3. Masliah E, DeTeresa RM, Mallory ME, Hansen LA. Changes in pathological findings at autopsy in AIDS cases for the last 15 years. *AIDS* 2000; **14**: 69–74.
4. Budka H, Willey CA, Kleihues P *et al.* HIV-associated disease of the nervous system: review of nomenclature and proposal for neuropathology-based terminology. *Brain Pathol* 1991; **1**: 143–152.
5. Budka H. Neuropathology of human immunodeficiency virus infection. *Brain Pathol* 1991; **1**: 163–175.
6. Budka H, Costanzi G, Cristina S *et al.* Brain pathology induced by infection with the human immunodeficiency virus (HIV). A histological, immunocytochemical, and electron microscopical study of 100 autopsy cases. *Acta Neuropathol* 1987; **75**: 185–198.
7. Raja F, Sherriff FE, Morris CS, Bridges LR, Esiri MM. Cerebral white matter damage in HIV infection demonstrated using beta-myeloid precursor protein immunoreactivity. *Acta Neuropathol* 1997; **93**: 184–189.
8. An SF, Giometto B, Groves M *et al.* Axonal damage revealed by accumulation of beta-APP in HIV-positive individuals without AIDS. *J Neuropathol Exp Neurol* 1997; **56**: 1262–1268.
9. Giometto B, An SF, Groves M *et al.* Accumulation of beta-amyloid precursor protein in HIV encephalitis: relationship with neuropsychological abnormalities. *Ann Neurol* 1997; **42**: 34–40.
10. Wiley CA, Achim CL, Christopherson C *et al.* HIV mediates a productive infection of the brain. *AIDS* 1999; **13**: 2055–2059.
11. Tyor WR, Glass JD, Griffin JW *et al.* Cytokine expression in the brain during the acquired immunodeficiency syndrome. *Ann Neurol* 1992; **31**: 349–360.
12. Wesselingh SL, Takahashi K, Glass JD, McArthur JC, Griffin JW, Griffin DE. Cellular localization of tumor necrosis factor mRNA in neurological tissue from HIV-infected patients by combined reverse transcriptase/polymerase chain reaction in situ hybridization and immunohistochemistry. *J Neuroimmunology* 1997; **74**: 1–8.
13. Canki M, Potash MJ, Bentsman G *et al.* Isolation and long-term culture of primary ocular human immunodeficiency virus type 1 isolates in primary astrocytes. *J Neurovirol* 1997; **3**: 10–15.
14. da Cunha A, Jefferson JJ, Tyor WR, Glass JD, Jannotta FS, Vitkovic L. Control of astrocytosis by interleukin-1 and transforming growth factor-beta 1 in human brain. *Brain Res* 1993; **631**: 39–45.
15. Canki M, Thai JN, Chao W, Ghorpade A, Potash MJ, Volsky DJ. Highly productive infection with pseudot-

yped human immunodeficiency virus type 1 (HIV-1) indicates no intracellular restrictions to HIV-1 replication in primary human astrocytes. *J Virol* 2001; **75**: 7925–7933.

16. Genis P, Jett M, Bernton EW *et al.* Cytokines and arachidonic metabolites produced during human immunodeficiency virus (HIV)-infected macrophages-astroglia interactions: implications for the neuropathogenesis of HIV disease. *J Exp Med* 1992; **176**: 1703–1718.
17. Gonzalez-Scarano F, Martin-Garcia J. The neuropathogenesis of AIDS. *Nat Rev Immunol* 2005; **5**: 69–81.
18. Murray EA, Rausch DM, Lendvay J, Sharer LR, Eiden LE. Cognitive and motor impairments associated with SIV infection in rhesus monkeys. *Science* 1992; **255**: 1246–1249.
19. Zink MC, Amedee AM, Mankowski JL *et al.* Pathogenesis of SIV encephalitis. Selection and replication of neurovirulent SIV. *Am J Pathol* 1997; **151**: 793–803.
20. Mori K, Ringler DJ, Kodama T, Desrosiers RC. Complex determinants of macrophage tropism in env of simian immunodeficiency virus. *J Virol* 1992; **66**: 2067–2075.
21. Xing HQ, Moritoyo T, Mori K *et al.* Simian immunodeficiency virus encephalitis in the white matter and degeneration of the cerebral cortex occur independently in simian immunodeficiency virus-infected monkey. *J Neurovirol* 2003; **9**: 508–518.
22. Brabers NA, Nottet HS. Role of the pro-inflammatory cytokines TNF-alpha and IL-1beta in HIV-associated dementia. *Eur J Clin Invest* 2006; **36**: 447–458.
23. Yeung MC, Pulliam L, Lau AS. The HIV envelope protein gp120 is toxic to human brain-cell cultures through the induction of interleukin-6 and tumor necrosis factor-alpha. *AIDS* 1995; **9**: 137–143.
24. Nicolini A, Ajmone-Cat MA, Bernardo A, Levi G, Minghetti L. Human immunodeficiency virus type-1 Tat protein induces nuclear factor (NF)-kappaB activation and oxidative stress in microglial cultures by independent mechanisms. *J Neurochem* 2001; **79**: 713–716.
25. Viviani B, Corsini E, Binaglia M, Galli CL, Marinovich M. Reactive oxygen species generated by glia are responsible for neuron death induced by human immunodeficiency virus-glycoprotein 120 in vitro. *Neuroscience* 2001; **107**: 51–58.
26. Corasaniti MT, Bagetta G, Rotiroti D, Nistico G. The HIV envelope protein gp120 in the nervous system: interactions with nitric oxide, interleukin-1beta and nerve growth factor signalling, with pathological implications in vivo and in vitro. *Biochem Pharmacol* 1998; **56**: 153–156.
27. Zhao ML, Kim MO, Morgello S, Lee SC. Expression of inducible nitric oxide synthase, interleukin-1 and caspase-1 in HIV-1 encephalitis. *J Neuroimmunol* 2001; **115**: 182–191.
28. Gray F, Scaravilli F, Everall I *et al.* Neuropathology of early HIV-1 infection. *Brain Pathol* 1996; **6**: 1–15.

Soluble PD-1 rescues the proliferative response of simian immunodeficiency virus-specific CD4 and CD8 T cells during chronic infection

Nattawat Onlamoon,[1,2*] Kenneth Rogers,[1*] Ann E. Mayne,[1] Kovit Pattanapanyasat,[2,3] Kazuyasu Mori,[4] Francois Villinger[1] and Aftab A. Ansari[1]

[1]*Department of Pathology & Laboratory Medicine, Emory University School of Medicine, Atlanta, GA, USA,* [2]*Division of Instruments for Research, Office for Research and Development, Faculty of Medicine Siriraj Hospital, Mahidol University, Bangkok, Thailand,* [3]*Thailand Research Fund (TRF) Senior Scholar, and* [4]*AIDS Research Center, National Institute of Infectious Diseases, Tsukuba Primate Research Center, National Institute of Biomedical Innovation 1 Hachimandai, Tsukuba, Japan*

doi:10.1111/j.1365-2567.2007.02766.x
Received 16 August 2007; revised 16 October 2007; accepted 25 October 2007.
*These authors contributed equally to this study.
Correspondence: Dr F. Villinger, 101 Woodruff Circle WMRB2307, Emory University School of Medicine, Atlanta, GA 30322, USA. Email: fvillin@emory.edu
Senior author: Dr A. A. Ansari, email: pathaaa@emory.edu

Summary

Phenotypic and functional studies of the programmed death-1 (PD-1) molecule on $CD4^+$ and $CD8^+$ T cells were performed on peripheral blood mononuclear cells from uninfected and simian immunodeficiency virus (SIV)-infected rhesus macaques. These data demonstrated a rapid upregulation of PD-1 expression on tetramer-positive $CD8^+$ T cells from MamuA.01$^+$ SIV-infected macaques upon infection. Upregulation of PD-1 on total $CD8^+$ T cells was not detectable. In contrast, $CD4^+$ T-cell PD-1 expression was markedly higher in total $CD4^+$ T cells during chronic, but not acute, infection and there was a correlation between the level of PD-1 expression on naive and central memory $CD4^+$ T cells and the levels of viral loads. Such association was emphasized further by a marked decrease of PD-1 expression on tetramer-positive CD8 T cells as well as on $CD4^+$ T cells on longitudinal samples collected before and after the initiation of antiretroviral therapy and downregulation of viral replication *in vivo*. Cloning of PD-1 and its two ligands from several non-human primate species demonstrated > 95% conservation for PD-1 and PD-L2 and only about 91% homology for PD-L1. Functional studies using soluble recombinant PD-1 protein or PD-1–immunoglobulin G fusion proteins induced marked increases in the SIV-specific proliferative responses of both $CD4^+$ and $CD8^+$ T cells from rhesus macaques. The results of these studies serve as a foundation for future *in vivo* trials of the use of rMamu-PD-1 to potentially enhance and/or restore antiviral immune responses *in vivo*.

Keywords: immune response; PD-1; PD-L1; simian immunodeficiency virus; T cells

Introduction

Both human and select non-human primate species infected with human immunodeficiency virus type 1 (HIV-1) and simian immunodeficiency virus (SIV), respectively, demonstrate a sequential progression of immune dysfunction which ultimately contributes to increased susceptibility to opportunistic infections and death.[1,2] While the time line for the appearance of such immune dysfunction varies, it is clear from following the initial depletion of $CD4^+$ T cells, primarily within the gastrointestinal tract,[3,4] that there is a gradual loss of CD28 expression, a failure of antigen-specific memory T cells to synthesize interleukin-2 (IL-2), to proliferate, to synthesize proinflammatory cytokines such as tumour necrosis factor-α, perforin, and interferon-γ (IFN-γ), and to degranulate, and a development of anergy followed by senescence and death.[5–12] The administration of antiviral chemotherapy in a variety of combinations has led to a dramatic decrease in viral loads and has prolonged the life of HIV-1-infected humans.[13–15] However, such chemotherapy is required for the lifetime of the patient; it is not without side effects and issues involving quality of life dictate that alternative strategies are desperately needed.[13,15–18] More importantly, such chemotherapy, while resulting in low to undetectable levels of plasma viraemia, does not appear to rapidly or fully reverse immune dysfunction.[17,19,20] Strategies for reconstituting immune function to a reasonably functional level have therefore been identified as one of the major research targets in lentiviral research.

Studies utilizing murine models of acute versus chronic infection, such as those that have used the lymphocytic choriomeningitis virus (LCMV) model system,

have provided significant new insights into the potential mechanisms of dysfunction of T-cell responses that occur during chronic viral infection.[21,22] Measurement of the kinetics of virus-specific immune function in such a model has shown that while robust virus antigen-specific functional T-cell responses can be measured during the acute infection period, this is soon followed by the progressive loss of such function during the chronic viraemia period and the T cells during such chronic viraemia have been termed 'immune exhausted'.[23,24] Such a lack of functional T-cell responses has also been described when antigen-specific T cells are repeatedly challenged with their cognate antigen, such as those described using the murine model of influenza virus infection.[25,26] These findings of 'immune exhaustion' in the murine system were remarkably similar to the observations made in a variety of human clinical infections, such as in patients with chronic hepatitis B or C virus infections and, more relevant to the present study, in HIV-1- and SIV-infected humans and non-human primates.[27–29] Until recently, the general consensus view was that such T-cell exhaustion was essentially non-reversible and the only avenue for successful replenishment of T-cell function was by the generation of newly minted T cells that should be provided with the right environment and growth potential *in vivo*. The only clinically applicable alternative reported so far has been the isolation of T cells from patients and non-human primates, followed by expansion *in vitro* and autologous adoptive transfer protocols.[30–32] Thus, the recent findings that blocking of the interaction between programmed death-1 (PD-1; CD279) and its cognate ligand PD-L1 can restore function in otherwise 'immune-exhausted' T cells has opened a new vista for the potential therapeutic utilization of such strategies *in vivo*.[21,33,34] It is important to note that before the discovery of the potential to reverse immune function by utilizing PD/PD-L1 blockade, similar strategies were explored for the blockade of cytotoxic T-lymphocyte antigen-4 with its ligands CD80/CD86,[35,36] blockade of B- and T-lymphocyte attenuator[37,38] and strategies aimed at manipulating regulatory T-cell function[39] in a variety of human diseases and animal models.

Our laboratory has been exploring strategies aimed at immune reconstitution in SIV-infected non-human primate models of acquired immune deficiency syndrome (AIDS).[40,41] Thus, rhesus macaques (*Macaca mulatta*) are susceptible to infection with SIV, a lentivirus that is highly related to HIV-1 and HIV-2, leading to chronic high viral loads, progressive immune dysfunction and immune exhaustion similar to human HIV infection.[42] A number of laboratories, including ours, have thus been contemplating studies aimed at determining whether the *in vivo* blocking of the PD/PD-L1 pathway leads to more robust SIV-specific immune responses and reversal of immune exhaustion in the rhesus macaques. However, it was reasoned that before embarking on such *in vivo* studies, a more detailed examination of the constitutive and induced expression of this molecule was warranted because the *in vivo* blocking of this pathway is likely to interfere with the normal physiological function of such interactions. The fact that SIV infection leads to the generation of a wide spectrum of autoantibodies,[43] which are known to be influenced by interactions between PD-1/PD-L1,[44,45] makes it important to take this issue into account if such *in vivo* studies are initiated. Finally, because the repeated use of monoclonal murine or even humanized antibodies against PD-1 or its ligand is bound to induce immune responses against the foreign antibodies in the monkeys and limit its use *in vivo* , our laboratory has prepared several recombinant forms of rhesus macaque PD-1 and herein report the efficacy of this reagent to enhance immune function in antigen-specific macaque peripheral blood mononuclear cells (PBMC) *in vitro*.

Materials and methods

Non-human primates

Ten adult healthy uninfected Indian rhesus macaques and 21 SIV-infected rhesus macaques served as blood donors for this study. All animals were housed at the Yerkes National Primate Research Center (YNPRC) of Emory University and were cared for in conformance with the guidelines of the Committee on the Care and Use of Laboratory Animals of the Institute of Laboratory Animal Resources, National Research Council and the Health and Human Services guidelines 'Guide for the Care and Use of Laboratory Animals'. The SIV-infected animals in these studies were inoculated intravenously with 200 50% tissue culture infective dose ($TCID_{50}$) of SIVmac239. The blood samples from these SIV-infected rhesus macaques were obtained at various times post-infection (p.i.). A sub-group of these rhesus macaques were treated with 9-(2-phosphonyl-methoxypropyly)adenine (PMPA) (20 mg/kg subQ daily for 28 days) after reaching viral load set-point and served as a source of samples for the study of the effect of antiviral drug therapy on the expression of PD-1. RNA samples from other species were obtained through the Resource for non-human primate immune reagents (http://pathology.emory.edu/Villinger/index.htm).

Viral load determination

Plasma viral load was routinely monitored in each of the SIV-infected monkey species by the NIAID, NIH CFAR sponsored Virology Core Laboratory of Emory University School of Medicine.

Flow cytometric analysis of PD-1

The PBMC were isolated from freshly obtained peripheral blood samples from each monkey using standard Ficoll–Hypaque gradient centrifugation. The cells at the interface were washed twice with RPMI-1640 supplemented with penicillin/streptomycin, L-glutamine and 10% fetal calf serum (hereafter referred to as media). The PBMC were adjusted to 10×10^6/ml media and dispensed in 100-μl aliquots into individual 5-ml sterile test tubes. Aliquots of the PBMC were then incubated with a predetermined optimum concentration of fluorescein iosthiocyanate (FITC)-conjugated anti-CD95, phycoerythrin (PE)-conjugated anti-CD28, Peridinin chlorophyll protein (PerCP)-conjugated anti-CD4 (or PerCP-conjugated anti-CD8) and biotinylated anti-PD-1 followed by allophycocyanin (APC)-conjugated streptavidin. Controls consisted of a tube that was incubated with similarly conjugated identical isotype immunoglobulin (background control), tubes with each of the above reagents alone, and a tube containing the same combination of reagents except biotinylated clone SP34 (anti-CD3) was utilized instead of biotinylated anti-PD-1 (to make sure that the frequencies of PD-1-expressing $CD4^+$ $CD8^+$ T cells reflected accurate frequencies of the CD4 and CD8 subsets). All the stained tubes were incubated for 30 min at 4°, washed three times with media and then resuspended in 0·5 ml cold phosphate-buffered saline (PBS) pH 7·4 containing 2% fetal bovine serum and then subjected to flow cytometric analysis using the fluorescence-acitvated cell sorting (FACS) Caliber (B-D immunocytometry Division, Mountain View, CA). Following standard gating using forward and side scatter for lymphoid cells, data on a minimum of 20 000 events were collected and the data obtained on the subsets were analysed utilizing CELL QUEST and FLOWJO software.

Analysis of PD-1 expression by p11c-tetramer-reagent-positive cells

Basically, the protocol was the same as above, except aliquots of the PBMC from Mamu-$A01^+$ monkeys were incubated with predetermined optimum concentrations of FITC-conjugated anti-CD3 (clone SP34, BD, Mountain View, CA), PE-conjugated p11c tetramer complex (courtesy of Dr John Altman, Emory University VRC, Atlanta, GA), PerCP-conjugated anti-CD8 and biotinylated anti-PD-1 followed by APC-conjugated streptavidin. Again, the tubes were washed twice in media and then resuspended in 0·5 ml cold PBS pH 7·4 + 2% fetal calf serum vortexed gently and then subjected to flow cytometric analysis as described above. The frequency of p11c-tetramer-positive cells that stained with the anti-PD-1 reagent was determined.

Quantification of cell proliferation

The effects of blocking the interaction between PD-1 and its ligand PD-L1 on virus antigen-specific T cells were analysed using a cell proliferation assay. Briefly, 10^7 PBMC were labelled with 5 μM carboxyfluorescein diacetate succinimidyl ester (CFSE), washed twice in PBS with 5% fetal bovine serum. The CFSE-labelled cells were adjusted to 1×10^6 cells/ml and incubated with either a mixture of SIV gag peptides covering the entire SIV gag sequence (20-mers overlapping by 12) at 0·1 μg/ml of each peptide or AT-2-treated SIVmac239 (containing 0·5 μg SIV p27) in media containing anti-CD28/CD49d monoclonal antibodies (1 μg/ml of each antibody) in the presence or absence of recombinant rhesus macaque PD-1 (rMamu-PD-1) at a predetermined optimal concentration of 6·7 μg/ml or 1–10 μg rMamu-PD-1–immunoglobulin G (IgG) or rMamu-PD-1–IgG mutant. The cells were cultured for 6 days and were maintained by the addition of fresh media on days 2 and 4. On day 6, the cells were stained with PE-conjugated anti-CD3,, PerCP-conjugated anti-CD4 and APC-conjugated anti-CD8. Proliferation was evaluated via dilution of CFSE on a FACS Calibur flow cytometer. Data from at least 50 000 cells gated on the lymphocyte population were analysed by FLOWJO software (Tree Star, Ashland, OR). $CD3^+$ cells were selected and the percentage of cells with diluted CFSE ($CFSE^{+low}$) was determined in gated populations of total $CD4^+$ or $CD8^+$ T cells.

Enumeration of SIV-specific T cells via IFN-γ ELISPOT

The enzyme-linked immunosorbent spot-forming cell (ELISPOT) assay was performed as previously described.[46] Briefly, the IFN-γ ELISPOT kit was a kind gift of Dr N. Ahlborg (Mabtech, Nacka, Sweden); this kit utilizes the clones GZ-4 and 7-B6-1 for the capture and detection of the cytokine. The assay was performed using unfractionated PBMC from the monkeys. Individual wells of the assay kit were incubated with 250 000 PBMC in complete media alone (negative control), 5 μg/ml concanavalin A (positive control), or 10 μg/ml of individual pools of overlapping SIV gag (each pool containing eight peptides which were 20-mers overlapping by 12) or env peptides (each pool containing eight peptide 25-mers overlapping by 13, courtesy of the NIH AIDS Reagent Program) and the plates were incubated overnight at 37° in a 7% CO_2 humidified incubator. Each culture was performed in the absence or presence of 10 μg/ml goat polyclonal anti-PD-1 (AF1086, R&D Systems, Minneapolis, MN) or the anti-PD-L1 (clone MIH1, eBioscience, San Diego, CA) monoclonal antibody. The wells were washed extensively, which was followed by the addition of the biotinylated detector antibody and incubation for 2 hr. The wells were once again washed and streptavidin-conjugated alkaline phosphatase was added, followed by the addition of the substrate nitro-

blue tetrazolium/5-bromo-4-chloro-3-indolylphosphate buffer (Mabtech). An automated spot reader system (CTL, Shaker Heights, OH) was used to determine the developed spots and the mean number of spots in the experimental wells was deducted from the media control to derive the net spots which were then used to calculate the average spot-forming cells per 10^6 input cells. In limited experiments, once a distinct pool of SIVenv or SIVgag was found to induce significant responses, PBMC from the same monkey were obtained at a later time interval and the assay was repeated using the same protocol with the cells being incubated with individual peptides of the pool in an effort to more clearly identify the role of PD/PD-L1 blockade on specific SIV peptide-specific responses.

Cloning and characterization of non-human primate PD-1, PD-L1 and PD-L2

Cloning of the PD-1 and its two ligands was performed by reverse transcription–polymerase chain reaction (RT-PCR) from RNA isolated from activated PBMC, lymph node cells or splenocytes from rhesus macaques (*Macaca mulatta*), sooty mangabeys (*Cercocebus atys*) and, for purposes of phylogenetic comparison, pigtailed macaques (*Macaca nemestrina*), cynomolgus macaques (*Macaca fascicularis*), baboon (*Papio anubis*) and the common marmoset (*Callithrix jacchus*) as previously described.[47] The primers were designed after blasting the human cDNA with the rhesus genome (http://www.hgsc.bcm.tmc.edu). The primers utilized included the following: (sense PD-1: CWCTGSTGGRGCTGCTCCAGG; anti-sense PD-1: TGA AGCAGTGACTGCATCTGG and CTCATGGTGGAGGG TCTGCAG; sense PD-L1: CGAGGCTCCGCACCAGCCG and TGCAGGGCATTCCAGAAGAT; anti-sense PD-L1: TTTCGCCAGGTTCCATTTTCAGTG and AATCCCTGC TTGAAGATCAGAAGT; sense PD-L2: CAGCTAGAAAG AATCCTGGGTT and GGCTGT TCATTTTGGTGGCTA; anti-sense CARGTTTCAGATTAAAGTGCTGG and CTG GCTCCCAAGACCACAGGT.

The amplified fragments were ligated into pGEM-T (Promega; Madison, WI) vectors. The ligated plasmids were transfected and amplified into competent JM109 cells. Plasmids were then purified and the various clones were sequenced (Agencourt, Beverly, MA). Several clones obtained from multiple animals from the same species were analysed and shorter amplicons were analysed for the evaluation of potential splice variants. The sequences were compared and aligned using the GCG package.

Construction and expression of recombinant soluble macaque PD-1 and soluble macaque PD-1–IgG fusion protein

In an effort to create antagonists to the PD-1–ligand pathways without the capacity to signal through either PD-1 or its ligands, recombinant soluble PD-1 was expressed. A fragment corresponding to the mature extracellular domain of rhesus macaque PD-1 was amplified with sense primer TGC*CCATGG*ACCAGGATGGTTCT TAGACTCC introducing an *Nco*I site for fusion with the macaque IL-4 leader peptide, and the anti-sense primer AGCATGC*GAATTC*AGTGGTGATGGTGATGGTGCACCA GGGCTTGGAACTGG binding to the C terminus of the extracellular domain of PD-1 fused to a hexahistidine tag. The amplified fragment was then ligated in frame with the macaque IL-4 leader sequence[47] and the entire insert was then subcloned into the pcDNA3.1 Neo(–) using *Sal*I and *Eco*RI. Expression was performed in transfected T293 with purification of the PD-1 released in the supernatants using a nickel activated column (Amersham Bioscience, Piscataway, NJ). After elution with 250 mM imidazole, the protein was dialysed against PBS and tested for purity by polyacrylamide gel electrophoresis and Coomassie staining as well as by Western blot.

In addition, because these antagonists were to be used *in vivo* with the need for longer half-lives and bioavailability, soluble rhesus PD-1 was also fused to either the native macaque IgG2 heavy chain Fc (consisting of the hinge region, CH2 and CH3 domains) or a mutant Fc. For the mutant Fc two amino acid substitutions were introduced to eliminate potential interactions with Fc receptors and complement, L235A and P331S, respectively.[48,49] Each construct was introduced into the pcDNA3.1 Neo(–) expression vector and production of the PD-1/Fc proteins was carried out in 293T cells transfected using the Amaxa system (Gaithersburg, MD). Expression vector construction was carried out using a series of PCRs to fuse the various fragments. Briefly, the extracellular domain of rhesus PD-1 in frame with the rhesus IL-4 leader sequence was amplified from pGEM rh4sPD-1 (his) with the primers T7 and PD-1Ig2b (5′-GTAGATCTACCCACCAGGGCTTGGA ACTG-3′) and the IgG2 Fc encoding fragment was produced by amplifying from the pGEM PAmIL15IgG plasmid using primers PAmigg2b (5′-GGTAGATCTACGTGC CCACCGTGCCCAGCTGAA-3′) and IgG6ae (5′-TATG ACGTCGAATTCTCATTTACCCGGAGACACGGAGA-3′). These two fragments were then joined by PCR using primers T7 and IgG6ae. The resulting product was digested with *Spe*I and *Eco*RI and ligated into pcDNA3.1 Neo(–) previously digested with *Nhe*I and *Eco*RI, resulting in pcDNA PD-1/Fc.

The mutant PD-1/Fc was similarly produced except that the pcDNA3.1 insert was constructed by the following series of PCRs to create the desired mutations. First, three overlapping PCR fragments were amplified: the 5′ end (encoding PD-1 fused to the N-terminal portion of the Fc) using primer T7 and G2L235AR (5′-TGACGG TCCCCCCGCGCGTTCAGCTGGGCA-3′); an internal 316-base pair (bp) fragment was amplified with primers G2L234AF (5′-AGCTGAACTCGCGGGGGGACCGTCAG

TCTT-3′) and P331SR (5′-ACAGTTTTCTGCCTTGAG GCCGGGAGGCCT-3′), and a 3′ end 383-bp fragment amplified with primers P331SF (5′-AGGCCTCCCGGCC TCAAGGCAGAAAACTGT-3′) and IgG6ae. The two fragments comprising the C terminus of the mutated IgG Fc were then reassembled using primers G2L234AF and IgG6ae and the resulting product was joined to the 5′ end containing the IL-4 leader, PD-1 soluble fragment fused to the hinge regions of the immunoglobulin using primers T7 and IgG6ae. All constructs were verified by sequencing.

PD-1–Ig was purified onto Sepharose Protein G columns, eluted with 0·2 N acetic acid/0·15 M NaCl pH 2·5, and neutralized with one-tenth 2 M Tris–HCl pH 9·5. The protein was dialysed against PBS and tested for purity by polyacrylamide gel electrophoresis and Coomassie staining as well as by Western blot.

Analysis of PD-1 mRNA by Northern blot

Briefly, aliquots of PBMC from human, rhesus macaque and sooty mangabey donors were either left unstimulated or stimulated overnight with beads coated with anti-CD3 (clone SP34 for human PBMC or FN18 for monkey PBMC) and anti-CD28 (clone L293) monoclonal antibodies or with 2 μg/ml of concanavalin A. After incubation the cells were washed and lysed and RNA was obtained using the Trizol reagent (Invitrogen, Carlsbad, CA). Ten-microgram aliquots of the various RNA samples were then run on an agarose gel and hybridized to a ^{32}P-labelled probe generated from the rhesus macaque PD-1 full-length clone via random primer labelling. After extensive washes, the blots were exposed to film for various lengths of time.

Statistical analyses

Data are presented as mean ± SD of the number of samples that were utilized for each of the assays or analyses. The Mann–Whitney *U*-test was utilized to calculate statistical significance using the STATVIEW software program (Cary, NC).

Results

Sequence analysis of PD-1, PD-L1 and PD-L2

In attempts to verify the homologies of PD-1 and its ligands PD-L1 and PD-L2 in our study model, each molecule was cloned from RNA isolated from the PBMC of several rhesus macaques and sooty mangabeys as well as from RNA samples isolated from the PBMC of a number of other non-human primate species. Several PD-1 cDNA clones were obtained from the Old World primate species *M. mulatta*, *M. fascicularis*, *M. nemestrina* and sooty mangabeys and sequenced (Fig. 1a). Overall, these sequences shared > 96% homology at both the nucleotide and amino acid levels. Most amino acid changes were conserved among the four Old World primate species analysed. Our cloning attempts for New World marmoset PD-1 was not successful. One clone each from a rhesus and a mangabey was missing a lysine residue at the beginning of Exon 5, which was reminiscent of a previously reported splicing event for the T-cell receptor zeta transcript, in which a G-protein motif appeared disrupted by the insertion of an additional residue at the junction right before an immunoreceptor tyrosine-based activation motif.[50] The deletion in these PD-1 clones does not *a priori* induce any detectable functional alteration. In fact both the intracellular immunoreceptor tyrosine-based inhibition and switch motifs were clearly conserved among the various primate species. Of interest also was the finding that a number of shorter open reading frames were identified that curiously did not conform to a strict exon/intron splicing event because both of the clones were missing part of exon 1, the entire exon 2 and part of exon 3, resulting in a deletion of most of the extracellular domain of PD-1. Such large deletions have been noted before for other molecules (e.g. T-cell immunoglobulin and mucin domain protein-3 (TIM-3) and refs 51,52) although the functional relevance of such transcripts remains unknown. Although alternative splice variants of human PD-1 have been reported,[51,53] the variants identified herein from both Old World primate species represent novel variants. To address the potential presence of alternative splice variants, Northern blot analysis of resting and activated PBMC was performed. Representative data from several such analyses are shown in Fig. 1b. There appeared to be at least two major variants that were detectable for humans and mangabeys and potentially three variants in rhesus macaques. It is not clear which of these variant(s) were finally expressed on the cell membrane in a functional form.

In addition to PD-1, its cognate ligands PD-L1 and PD-L2 were also cloned and sequenced. While the degree of conservation of PD-L1 was relatively high at the nucleotide level (96%) across the various primate species tested, at the protein level, 7–10% divergence was noted between monkey and human PD-L1 (Fig. 1c). Of note, and as previously reported,[47] the New World marmoset sequence was approximately equidistant in divergence between human and Old World primates. The sequences derived from cynomologus macaques and from a baboon exhibited an early termination signal and may not have been representative of the species. Also of interest was the isolation of a deletion construct comprising essentially only the extracellular immunoglobulin-like V-type domain. It is possible that if such a sequence is synthesized it is likely to be in a soluble form and has the potential to bind to PD-1. This clone was however only obtained from a single animal and it remains to be